THE JOURNAL OF BIOLOGICAL CHEMISTRY VOL. 290, NO. 11, pp. 7247–7258, March 13, 2015

Paraoxonase 2 Serves a Proapopotic Function in Mouse and Human Cells in Response to the *Pseudomonas aeruginosa* Quorum-sensing Molecule *N*-(3-Oxododecanoyl)-homoserine Lactone*

Received for publication, October 19, 2014, and in revised form, January 6, 2015 Published, JBC Papers in Press, January 27, 2015, DOI 10.1074/jbc.M114.620039

Christian Schwarzer[‡], **Zhu Fu**[‡], **Takeshi Morita**[‡], **Aaron G. Whitt**[§], **Aaron M. Neely**[§], **Chi Li**[§], **and Terry E. Machen**[‡1]

From the [‡]*Department of Molecular and Cell Biology, University of California at Berkeley, Berkeley, California 94720-3200 and the* [§]*Departments of Medicine, Pharmacology, and Toxicology, Molecular Targets Program, James Graham Brown Cancer Center, University of Louisville, Louisville, Kentucky 40202*

Background: *Pseudomonas aeruginosa* use *N*-(3-oxododecanoyl)-homoserine lactone (C12) for intercellular communication; paraoxonase 2 (PON2) is an animal enzyme that cleaves lactones.
Results: C12 elicited apoptosis in mouse and human cells expressing PON2 with intact lactonase activity but not in cells without it.
Conclusion: PON2 mediates C12-induced apoptosis in mammalian cells.
Significance: PON2 in host cells hydrolyzes C12 and promotes C12-induced apoptosis.

Pseudomonas aeruginosa **use quorum-sensing molecules, including *N*-(3-oxododecanoyl)-homoserine lactone (C12), for intercellular communication. C12 activated apoptosis in mouse embryo fibroblasts (MEF) from both wild type (WT) and Bax/Bak double knock-out mice (WT MEF and DKO MEF that were responsive to C12, DKO_R MEF): nuclei fragmented; mitochondrial membrane potential ($\Delta\psi_{mito}$) depolarized; Ca^{2+} was released from the endoplasmic reticulum (ER), increasing cytosolic [Ca^{2+}] (Ca_{cyto}); and caspase 3/7 was activated. DKO_R MEF had been isolated from a nonclonal pool of DKO MEF that were non-responsive to C12 (DKO_{NR} MEF). RNAseq analysis, quantitative PCR, and Western blots showed that WT and DKO_R MEF both expressed genes associated with cancer, including paraoxonase 2 (*PON2*), whereas DKO_{NR} MEF expressed little *PON2*. Adenovirus-mediated expression of human PON2 in DKO_{NR} MEF rendered them responsive to C12: $\Delta\psi_{mito}$ depolarized, Ca_{cyto} increased, and caspase 3/7 activated. Human embryonic kidney 293T (HEK293T) cells expressed low levels of endogenous PON2, and these cells were also less responsive to C12. Overexpression of PON2, but not PON2-H114Q (no lactonase activity) in HEK293T cells caused them to become sensitive to C12. Because [C12] may reach high levels in biofilms in lungs of cystic fibrosis (CF) patients, PON2 lactonase activity may control $\Delta\psi_{mito}$, Ca^{2+} release from the ER, and apoptosis in CF airway epithelia. Coupled with previous data, these results also indicate that PON2 uses its lactonase activity to prevent Bax- and Bak-dependent apoptosis in response to common proapoptotic drugs like doxorubicin and staurosporine, but activates Bax- and Bak-independent apoptosis in response to C12.**

Pseudomonas aeruginosa is a ubiquitous bacterium present in the soil and water. *P. aeruginosa* is also an opportunistic pathogen that infects patients with the genetic disease cystic fibrosis (CF)[2] and also patients with burns or compromised immune functions. *P. aeruginosa* use *N*-(3-oxododecanoyl)-homoserine lactone (C12) and *N*-(3-oxobutyryl)-homoserine lactone (C4), so-called quorum-sensing molecules, to communicate with each other by activating the lasI/rhlI and lasR/rhlR regulatory gene networks (1–3). Activation of these regulatory genes leads to production of biofilms, masses of very large numbers and densities of bacteria ($>10^9$ cfu/ml), which are encased in a matrix of polysaccharides and DNA and other components and that are extremely difficult to clear (4–6). Although concentrations of C12 in the airway surface liquid remain debated, there is some evidence indicating that the concentrations of the quorum-sensing molecules may reach high micromolar concentrations in or adjacent to biofilms (7–9).

C12, but not C4, also has multiple effects on host cells. Because it is lipid-soluble and membrane-permeant (10), C12 is likely capable of affecting all the cells near high densities of *P. aeruginosa* occur. In the lung airways this will include the airway epithelial cells, macrophages, neutrophils, fibroblasts, and endothelial cells lining nearby capillaries and smooth muscle cells in the serosa. C12 elicits increased expression (*i.e.* gene transcription) of proinflammatory mediators like IL8 (11, 12). However, C12 also causes reduced secretion of these same proinflammatory mediators (13–16). Recent work showed that these contradictory effects may be mediated through the effects

* This work was supported, in whole or in part, by National Institutes of Health Grants PN2-EY-018241, R01AM10141, K01CA106599, P20RR018733, and R01 CA175003, Cystic Fibrosis Research, Inc. (New Horizons), and a Research Initiation Grant from the University of Louisville.

[1] To whom correspondence should be addressed: 231 LSA, University of California, Berkeley, CA 94720-3200. Tel.: 510-642-2983; Fax: 510-643-6791; E-mail: tmachen@berkeley.edu.

[2] The abbreviations used are: CF, cystic fibrosis; C12, *N*-(3-oxododecanoyl)-homoserine lactone; C4, *N*-(3-oxobutyryl)-homoserine lactone; PON, paraoxonase; FCCP, carbonyl cyanide-4-(trifluoromethoxy)phenylhydrazone; $\Delta\psi_{mito}$, mitochondrial membrane potential; Ca_{cyto}, cytosolic Ca^{2+} concentration; DKO_R MEF, fibroblasts from Bax/Bak double-knockout ($Bax^{-/-}$/$Bak^{-/-}$) mice that were responsive to C12; DKO_{NR} MEF, DKO MEF that did not respond to C12; PI, propidium iodide; Z, benzyloxycarbonyl; fmk, fluoromethyl ketone; Q-PCR, quantitative PCR; BisTris, 2-[bis(2-hydroxyethyl)amino]-2-(hydroxymethyl)propane-1,3-diol.

of C12 to cause release of Ca^{2+} from the ER, triggering ER stress and the ER stress-regulated kinase PERK, activation of IRE1α, phosphorylation of eIF2a, and inhibition of protein (including cytokine and IκB) synthesis and secretion (16). C12 also triggers apoptosis in multiple cell types (9, 17–21). That C12 activates apoptosis and not some other type of cell death has been documented from the multiple responses that are classically attributed to apoptosis: membrane blebbing, nuclear condensation and fragmentation, depolarization of mitochondrial membrane potential ($\Delta\psi_{mito}$), release of cytochrome *c* from mitochondria into the cytosol, and activation of caspases 3/7, 8, and 9 and block by the pan-caspase inhibitor Z-VAD-fmk (9, 22). A unique aspect of C12-triggered apoptosis was that it occurred equally well in fibroblasts from wild type mouse embryos and from Bax/Bak double knock-out ($Bax^{-/-}/Bak^{-/-}$) mouse embryos (DKO MEF) (23). In the present paper we refer to these Bax/Bak double knock-out DKO MEF that were responsive to C12 as DKO_R MEF. The molecular mechanisms involved in C12-triggered apoptosis have not been determined, but Haggie and colleagues (21) showed that activation of caspases and cell death required IRE1α, splicing of XBP1, and production of XBP1s.

Although C12 causes apoptosis, ER stress, and altered inflammatory signaling and responses in many different types of cells in *in vitro* studies, it has been difficult to determine the physiological relevance of these effects, particularly whether *P. aeruginosa* secrete high enough concentrations of C12 to cause its characteristic responses. This apparent contradiction may result from the fact that airway and intestinal epithelia, both of which may be exposed to large numbers of *P. aeruginosa* under pathological conditions, express paraoxonase 2 (PON2) that has lactonase activity and can cleave C12 (24, 25). It has been proposed that this cleavage reduces quorum sensing by the bacteria. This lactonase activity might also be expected to reduce effects of C12 on PON2-expressing cells.

PON2 is part of a gene family (PON1, PON2, and PON3) that has Ca^{2+}-dependent (26–28) lactonase and arylesterase activities (26–30). PON2 and PON3 appear also to serve antioxidant, anti-inflammatory, anti-ER stress, and anti-apoptotic functions (31, 32). PON2 and PON3 are highly expressed in multiple cancers (33–37), and overexpression of PON3 protects against mitochondrial-triggered apoptosis (38–40). Importantly, inactivation of the lactonase activity of PON2 (using PON2(H114Q) (41) does not alter its ability to prevent cellular oxidation, and PON2(H114Q) appears to be more effective than wild type PON2 in preventing apoptosis in response to the common proapoptotic agonists staurosporine, doxorubicin, and tunicamycin. Although the mechanism used by PON2 to prevent apoptosis has not been determined, it is clear that PON2 has independent lactonase and anti-apoptotic functions (41).

During our recent study of DKO_R MEF (23) we discovered that the uncloned pool of DKO MEF from which DKO_R were isolated were non-responsive to C12, we called them DKO_{NR} MEF. This paper first compares the Bax and Bak phenotypes and then caspase 3/7 responses of WT, DKO_R, and DKO_{NR} MEF. We then report results from RNAseq, Q-PCR, and Western blot analysis of the WT, DKO_R, and DKO_{NR} MEF. Although the DKO_R MEF were isolated from the DKO_{NR} MEF, RNAseq identified more than 5000 genes that were different between the two cell lines. By further comparison of WT and the two DKO lines, we identified PON2 as a gene of interest, although its expression was opposite from what might have been expected: DKO_{NR} MEF expressed very low levels of PON2 mRNA and had protein below detection limits, whereas WT and DKO_R MEF both expressed high levels of PON2 mRNA and protein. We then tested whether adenoviral-mediated expression of human PON2 in DKO_{NR} MEF caused them to become responsive to C12 in the apoptosis assays. We also tested the roles of PON2 *versus* PON2(H114Q) in C12-triggered apoptosis in human embryonic kidney (HEK293T) cells, which we found expressed only low levels of PON2 but could be transduced to stably express PON2 and PON2(H114Q) using a retrovirus infection approach.

EXPERIMENTAL PROCEDURES

Reagents—Unless otherwise specified, reagents and chemicals were obtained from Sigma. C12 was dissolved in dimethyl sulfoxide and frozen in separate vials, and then thawed for single experiments. JC1 and fura-2 were both purchased from Invitrogen and dissolved in dimethyl sulfoxide at 10 mM. Dyes were then diluted into solutions to give concentrations mentioned in the text. Anti-mouse PON2 were obtained from Antibodies-on-Line, Atlanta, GA, and anti-human PON2 from Abcam, Cambridge, MA.

Mouse Embryo Fibroblasts—Wild type (WT) and an uncloned population of $Bak^{-/-}Bax^{-/-}$ (DKO) MEF immortalized by SV40 large T antigen expression have been described previously (23, 42). DKO MEF cells were resistant to many proapoptotic stimuli. These DKO cells were not responsive to C12 and were termed DKO_{NR} MEF. Single clonal cell lines of the DKO MEFs were acquired from the DKO_{NR} by limited dilution. One DKO clone was selected for its ability to resist various proapoptotic stimuli. This line was termed DKO_R MEF because these cells responded to C12, as described in our previous publication (23). WT, DKO_R, and DKO_{NR} MEF were cultured in DMEM/high glucose medium (Mediatech, Manassas, VA) with 10% (v/v) fetal bovine serum (Gemini, West Sacramento, CA), 100 units ml^{-1} of penicillin, and 100 μg ml^{-1} of streptomycin (Mediatech). Cells were grown in a humidified 95/5% air/CO_2 incubator at 37 °C. The cells were passaged at 1:5–1:10 dilutions and the remaining cell suspension was seeded directly onto 96-, 24-, or 12-well tissue culture plates (BD Falcon, Bedford, MA) or onto coverglasses for imaging.

Human Embryonic Kidney 293T Cells—HEK293T cells (ATCC, Bethesda MD) were obtained from the laboratory of Prof. E. Isacoff (University of California, Berkeley) and grown and passaged using methods as described above for MEF.

Adenoviral Expression of PON2—Adenovirus for EGFP, human CFTR, and human PON2 (hPON2) were obtained from the Gene Transfer Vector Core, University of Iowa. MEF were infected with 100 multiplicity of infection for 12 h, washed in medium, and used for experiments after 48 to 72 h post-adenoviral infection.

Cell Viability Assay—MEF cells were plated in 48-well tissue culture plates at the density of 2×10^4 cells/well for 24 h. The

indicated cell lines were treated with C12 or etoposide. Twenty-four hours later, cells were collected in the presence of 1 μg/ml of propidium iodide (PI) and the percentage of live cells was measured by a PI exclusion method using flow cytometry analysis (FACScalibur, Beckon Dickinson, San Jose, CA) as described previously (23).

Retroviral Re-expression of Bak or Bax—Murine *Bak* cDNA or murine *Bax* cDNA was cloned into the retroviral expression vector pBABE-IRES-GFP with enhanced green fluorescent protein (EGFP) expressing from an internal ribosomal entry site (IRES). For retrovirus production, human embryonic kidney (HEK)-293T was transfected with the empty vector or the retroviral plasmid carrying the particular gene of interest along with helper plasmids pUVMC and pMDG2.0 using the jetPRIME® transfection reagent (Polyplus-transfection, New York, NY). Retroviral supernatant was collected 48–72 h after transfection with the addition of 10 μg/ml of Polybrene (Sigma) to increase infection efficiency. Bak, Bax, Bak and Bax, or the control GFP alone was expressed in DKO_{NR} MEF by retroviral infection. The expression of Bak and Bax was determined by Western blot.

Sample Preparation and RNA Sequencing—WT, DKO_R, and DKO_{NR} MEF were grown to confluence in 12-well plates (~1 million cells/well; two wells of each cell line were used for RNAseq and Q-PCR analysis). Total RNA was isolated using TRIzol. RNA quality was assessed with the Agilent Bioanalyzer 2100 at the Functional Genomics Laboratory in University of California, Berkeley, and samples with RIN scores above 9 were used for cDNA production. One microgram of total RNA was used to isolate poly(A) purified mRNA, which was used for library construction by the Functional Genomics Laboratory. The average fragment sizes were ~400 bp. The library was sequenced with Ilumina HiSeq 2500 and each sample yielded 25 to 29 million 100-bp pair-end reads.

RNA Sequencing Read Alignment—RNAseq reads were mapped to the mouse reference genome (UCSC/mm9) using Tophat (43), and HTSeq (44) was used to sum the mapped reads to obtain gene expression levels. Read counts were normalized and differential expression between each sample pair was determined using DEseq (45). p value cutoff at $p < 0.01$ was used to define differential expression.

Retroviral Expression of PON2—The cDNA of wild type *hPON2* was acquired from Origene (Rockville, MD), and the cDNA of *hPON2* with the H114Q mutation was generated by gene synthesis (Biomatik, Wilmington, DE). Each cDNA was cloned into the retroviral expression vector pBabe-puro. The identity of the plasmids was confirmed by sequencing. To generate retrovirus, HEK293T cells were transfected with the empty vector or pBabe-puro carrying wild type *PON2* or *PON2*(*H114Q*) as well as the helper plasmids (pUVMC and pMDG2.0) using the jetPRIME® transfection reagent. Medium containing retrovirus was obtained 48–72 h following transfection with 10 μg/ml of Polybrene added to the medium to enhance infection efficiency. HEK293T cells stably expressing wild type PON2 or PON2(H114Q) were acquired by retroviral infection and culturing the cells in medium containing 1 μg/ml of puromycin. PON2 expression was examined by Western blot.

Q-PCR Analysis of Mouse Bax and Bak and Mouse and Human PON2—MEF were 12-well plated at 10^4 per well and grown for 3 days, left untreated, or infected with adenovirus expressing GFP (use as control) or human PON2 at 18 h after plating, then grown for another 48 h. When the cells reached >90% confluence, TRIzol reagent (Life Technologies) was applied to lyse the cells, and total RNA was extracted from the lysate per the manufacturer's protocol. RNA samples were treated with DNase (Frementas, Glen Burnie, MD) and reverse transcribed using SuperScript III (Invitrogen) with random primers. Mouse *Bax*, mouse *Bak1*, mouse *PON2*, and human *PON2* gene expression levels were determined by real-time PCR on triplicates carried out in a 7900HT Fast Real-time PCR System (Applied Biosystems) with SYBR mixture (KAPA Biosystems, Woburn, MA) using gene-specific primers. The housekeeping gene *Rps17* was used as normalization control throughout all experiments, and all data are presented as relative quantification score relative to *RPS17*. Primers used for real-time PCR were: mouse *Bax*, forward, 5′-TGAAGACAGGGGCCTTTTTG-3′ and reverse, 5′-AATTCGCCGGAGACACTCG-3′; mouse *Bak1*, forward, 5′-CAACCCCGAGATGGACAACTT-3′ and reverse, 5′-CGTAGCGCCGGTTAATATCAT-3′; mouse *PON2*, forward, 5′-CAGGGAGTGTGGTAAACAGG-3′ and reverse, 5′-ACTCCCCGGATTTTGATTAG-3′; human *PON2*, forward, 5′-CATCTGGGTAGGCTGTCATC-3′and reverse, 5′-TTGGAGAACAGACCCATTGT-3′; *Rps17*, forward, 5′-CGCCATTATCCCCAGCAAG-3′ and reverse, 5′-TGTCGGGATCCACCTCAATG-3′.

Western Blots—Whole cell lysates with an equal number of cells (5×10^4) were loaded on a 4–12% BisTris gel (Bio-Rad) and transferred onto PVDF membrane (Millipore). The membrane was incubated with the appropriate primary or secondary antibodies either at 4 °C overnight or at room temperature for 3 h in blotting buffer (1× PBS + 0.2% Tween 20) with 10% (w/v) nonfat dry milk (Bio-Rad). Protein levels were detected using the enhanced chemiluminescent detection system (Pierce). Antibodies used for Western blot analysis were anti-β-actin mAb (Sigma), anti-Bak pAb (Enzo, Farmingdale, NY), anti-Bax pAb (Santa Cruz Biotechnology, Santa Cruz, CA), anti-mouse PON2 (Antibodies-on-line), and anti-human PON2 (Abcam). Western blots were quantitated using densitometry (ImageJ; NIH, Bethesda, MD) by measuring the intensity of PON2 bands relative to actin, and then calculating the ratio of PON2/actin in PON2-expressing MEF or HEK293T cells to PON2/actin in parental cells.

Assay for Caspase 3/7—Caspase 3/7 activities were measured by cell-based homogeneous luminescent assays (Caspase-Glo, Promega, Madison, WI), in which a specific substrate that contains the tetrapeptide DEVD (specific for caspase 3/7) was cleaved by the activated caspases from the cells to release aminoluciferin reacting with the luciferase and resulting in the production of light (9, 23). WT and DKO MEF and HEK293T cells were plated on a clear-bottom, white 96-well plate in 100 μl of medium per well for 3–4 days until they were confluent. For the cells that were infected with adenovirus, the infection was done at 18 h after the cells were plated and then the cells were left to grow another 48 h. During the experiment, cells were treated with C12 in the

37 °C incubator for 120 min or left untreated as controls. On the same plate, some wells without cells but 100 μl of the same medium served as blanks. After treatment, 100 μl of reagent was added to each well with cells (treated or controls) and their medium, or blank (media only). The plate was incubated at room temperature for 1 h on a shaker, and the end point luminescence was measured in a plate-reading luminometer (LmaxII 384, Molecular Devices, Sunnyvale, CA). Data were background (blank) subtracted and averaged.

Imaging Measurements of $\Delta\psi_{mito}$ and Ca_{cyto}—For measurement of $\Delta\psi_{mito}$, MEF or HEK293T cells were incubated with medium containing the probe JC-1 (10 μM) for 10 min at room temperature and then washed three times with Ringer solution. The Ringer solution had the following composition (in mM): 145 NaCl, 5 KCl, 1.2 NaH_2PO_4, 5.6 glucose, 2.0 $CaCl_2$, 1.2 $MgCl_2$, and 10 HEPES, pH 7.4. Dye-loaded cells were mounted onto a chamber on the stage of a wide-field or a confocal imaging microscope and maintained at room temperature. Treatment consisted of diluting stock solutions into Ringer solution. Control experiments showed that equivalent amounts of dimethyl sulfoxide (0.1%) used to dissolve C12 did not affect the JC-1 signal. Real-time imaging measurements of $\Delta\psi_{mito}$ were performed using equipment and methods that have been reported previously (9). Briefly, a Nikon Diaphot inverted microscope with a ×40 Neofluar objective (1.4 numerical aperture) was used. A charge coupled device camera collected JC-1 emission images (green, 510–540 nm; red, 580–620 nm) during excitation at 490 ± 5 nm using filter wheels (Lambda-10, Sutter Instruments, Novato, CA). Axon Imaging Workbench 4.0 (Axon Instruments, Foster City, CA) controlled the filters and collection of data. Images were corrected for background (region without cells). Under control conditions, mitochondria exhibited red and green fluorescence of JC-1. C12 and the protonophore FCCP (10 μM) caused reductions of JC-1 red fluorescence and increases in JC-1 green fluorescence consistent with depolarization of mitochondria. When cells were treated with FCCP to elicit maximal depolarization of $\Delta\psi_{mito}$, JC-1 red fluorescence decreased to very low levels, and JC-1 green fluorescence increased to maximal intensity until the dye leaked out of the cytosol into the bath solution. Quantitative data are reported as fluorescence intensities normalized to minimal JC1 ratios obtained at the start of the experiment and maximal JC1 ratios obtained after treatment with 10 μM FCCP.

For measurements of cytosolic Ca^{2+} (Ca_{cyto}) cells grown on cover glasses were incubated with growth medium containing 2 μM fura-2/AM for 40–60 min at room temperature and then washed three times with Ringer solution. Fura-2-loaded cells were mounted onto a chamber on the stage of the imaging microscope and maintained at room temperature. Treatments with agonists were made by diluting stock solutions into Ringer solution at the concentrations stated in the text. Fluorescence ratio imaging measurements of Ca_{cyto} were performed using equipment as described above and methods reported previously (46, 47). Emission (>510 nm) images were collected during alternate excitation at 350 ± 5 and 380 ± 5 nm. Images were corrected for background (region without cells), and 380:350 ratios (a measure of Ca_{cyto}) were normalized to the maximal value obtained in 10 mM $CaCl_2$ Ringer's + 10 μM ionomycin and minimal values obtained in Ca^{2+}-free Ringer's + 100 μM EGTA + 10 μM ionomycin at the end of each experiment (48).

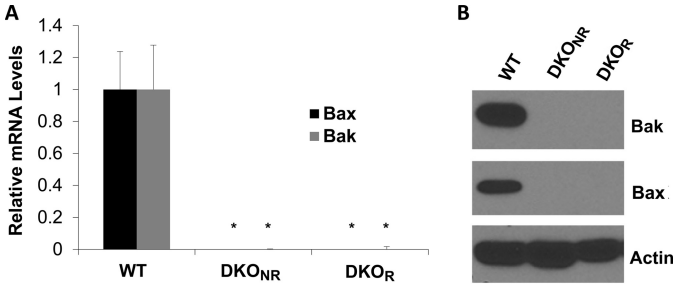

FIGURE 1. **Expression of Bak and Bax in WT but not in DKO_{NR} or DKO_R MEF.** *A,* Q-PCR. *B,* Western blot. *, $p < 0.05$ *versus* WT. Data are typical of three different experiments.

RESULTS

Characterization of DKO_{NR} MEF—Previous experiments (23) showed: (i) WT MEF expressed Bax and Bak, whereas DKO_R MEF did not. (ii) DKO_R and WT MEF were equivalently sensitive to C12 in terms of depolarization of $\Delta\psi_{mito}$, release of cytochrome *c* from mitochondria, activation of caspases and cell death. It was concluded that C12 triggered Bax and Bak-independent apoptosis in DKO_R MEF, a unique process that included release of cytochrome *c* from mitochondria.

During the course of those previous experiments, we discovered that the original pool of DKO MEF from which the clone of DKO_R MEF was isolated (23) was non-responsive to C12. We termed these DKO_{NR} MEF. As shown from Q-PCR and Western blot analyses (Fig. 1, *A* and *B*), both DKO_{NR} and DKO_R MEF were similar in that they expressed no detectable Bax or Bak, whereas WT MEF did. As reported previously (23), DKO_R MEF were relatively unaffected by the common proapoptotic stimulants staurosporine and etoposide, and retroviral-mediated expression of Bak or Bax or both Bak and Bax rendered them sensitive to staurosporine and etoposide. DKO_{NR} MEF ± Bax and/or Bak expression behaved similarly in their responses to staurosporine and etoposide (Fig. 2, *A* and *B*).

DKO_{NR} and DKO_R MEF were similar in that both showed low responses to conventional proapoptotic stimuli except following transfection with Bax or Bak. However, they behaved very differently from each other in their responses to C12. C12 increased caspase 3/7 activity and caused cell death (PI uptake) in WT and DKO_R MEF (23), but C12 had no effect on DKO_{NR} MEF (Fig. 3, *A* and *B*). C12 also had no effect on activating caspase 3/7 or cause PI uptake in DKO_{NR} MEF that had been transduced with the retrovirus to express Bax, Bak, or Bax + Bak (data not shown).

RNAseq Analysis of WT, DKO_R, and DKO_{NR} MEF—One potential explanation for the fact that C12 triggered apoptosis in DKO_R but not in DKO_{NR} MEF was that DKO_{NR} MEF did not express key gene(s) required for the action of C12. We performed RNAseq analysis to identify differences in expression (transcription) of DKO_R and DKO_{NR} MEF, and also included WT MEF for comparison.

Results from these experiments are presented in the Venn diagram in Fig. 4 and in Table 1. Of the 14,303 expressed genes,

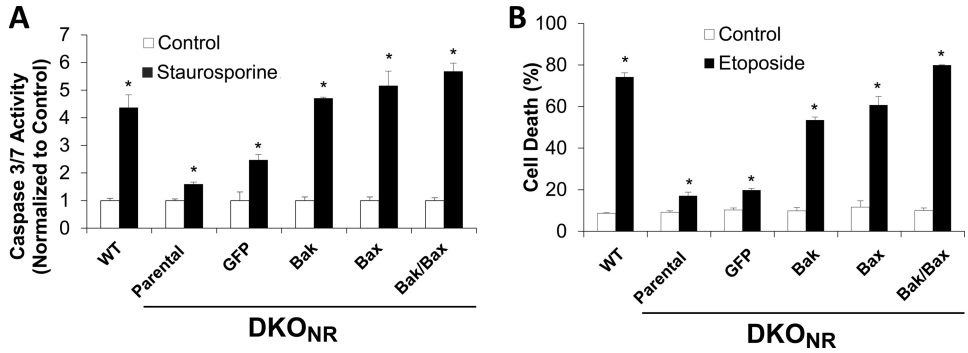

FIGURE 2. **Staurosporine and etoposide activation of apoptosis requires Bak or Bax expression in MEF.** *A*, DKO$_{NR}$ MEF or DKO$_{NR}$ MEF retrovirally re-expressing GFP, Bak, Bax, or Bak + Bax were left untreated or were incubated with staurosporine (10 μM) for 2 h, followed by assay for caspase 3/7 activity. Data are averages ± S.D. ($n = 3$). *B*, DKO$_{NR}$ MEF or DKO$_{NR}$ MEF retrovirally re-expressing GFP, Bak, Bax, or Bak + Bax were left untreated or incubated with etoposide (10 μM) for 24 h, then exposed to PI and processed by FACS to measure cell viability. *, $p < 0.05$ *versus* control.

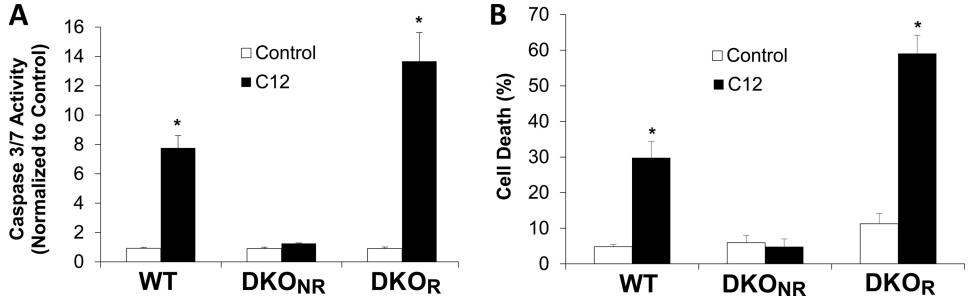

FIGURE 3. **C12 induces apoptosis in WT and DKO$_R$, but not DKO$_{NR}$ MEF.** *A*, WT, DKO$_{NR}$, and DKO$_R$ MEF were left untreated (control) or treated with C12 (50 μM) for 2 h followed by processing for caspase 3/7 activity. Data are averages ± S.D. ($n = 3$). *B*, WT, DKO$_{NR}$ and DKO$_R$ MEF were left untreated (control) or treated with C12 (100 μM) for 24 h, followed by adding PI and processing in the FACS. *, $p < 0.05$ *versus* control.

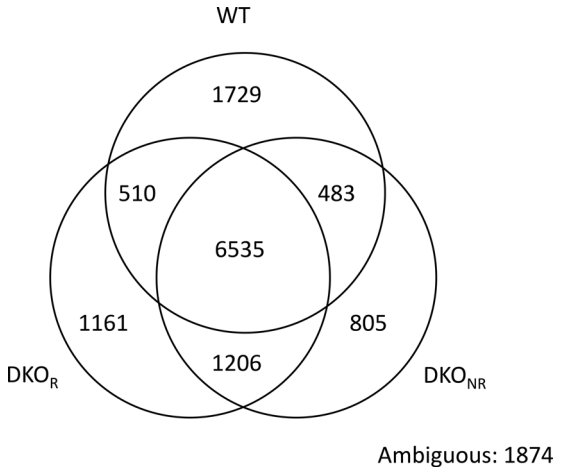

FIGURE 4. **RNAseq summary of gene expression in WT, DKO$_{NR}$, and DKO$_R$ MEF.** Numbers of genes expressed differently in the different groupings are shown.

a total of 8407 genes were expressed above background in WT, DKO$_R$, and DKO$_{NR}$ MEF (Fig. 4). 1729 were expressed selectively in WT, 805 were expressed selectively in DKO$_{NR}$, and 1161 were expressed selectively in DKO$_R$. Thus, both DKO$_R$ and DKO$_{NR}$ MEF had different gene expression profiles from WT MEF, and DKO$_R$ and DKO$_{NR}$ MEF also had different gene expression profiles from each other, even though clonal DKO$_R$ MEF were isolated from uncloned DKO$_{NR}$ MEF.

Because WT and DKO$_R$ MEF both responded to C12, whereas DKO$_{NR}$ MEF did not, we reasoned that candidate genes that were required for C12 to trigger apoptosis would be one of the 510 genes expressed in both WT and DKO$_R$ MEF but not in DKO$_{NR}$ MEF (Fig. 4). Many of the genes that exhibited the most significant differences between WT and DKO$_R$ MEF on the one hand and DKO$_{NR}$ MEF on the other (Table 1) were associated with cancer and/or growth regulation. Among these cancer-related genes, PON2 exhibited the most significantly different expression in DKO$_R$ MEF (high expression) compared with DKO$_{NR}$ MEF (low expression) (Table 1). PON3, which is thought to have similar antioxidant, anti-inflammatory, and anti-apoptotic functions as PON2 (31, 32), ranked 10 in this category of genes that exhibited the most significantly different expression in DKO$_R$ MEF *versus* DKO$_{NR}$ MEF. PON1 was not detected in MEF (0 mapped reads in all sequenced samples). Because PON2 hydrolyzes lactones including C12 (25–30), it was unexpected that PON2 was expressed at high levels in WT and DKO$_R$ MEF, which are sensitive to C12, but at low levels in DKO$_{NR}$ MEF, which are nonresponsive to C12. Although PON2 and PON3 would be expected to reduce, not enhance, proapoptotic effects of C12, there were reasons to think that previously unrecognized C12-PON2 interactions might be involved in the apparent proapoptotic effects of PON2 and therefore would be worth pursuing. For example, PON2 might cleave C12 into a potent proapoptotic molecule or C12 may inhibit the antiapoptotic activity of PON2 (49). We focused on PON2 for the rest of this study.

RNAseq data were confirmed by measuring expression of PON2 in the MEF. Results from Q-PCR (Fig. 5*A*) and Western blots (Fig. 5*B*) confirmed RNAseq data showing that PON2 was expressed at high levels in WT and DKO$_R$ MEF and at low levels in DKO$_{NR}$ MEF.

TABLE 1

Genes expressed in WT and DKO_R MEF but not in DKO_{NR} MEF

The 510 genes that were expressed in DKO_R and WT MEF but not in DKO_{NR} MEF were ranked in order of highest → lowest significance (based on *p* values). The top 25 genes (based on comparison of DKO_R *versus* DKO_{NR}, listed as symbols and names) are listed here. Statistical significances (*p* values) are listed for comparisons of DKO_R *versus* DKO_{NR}, WT *versus* DKO_{NR}, and WT *versus* DKO_R. *PON2* exhibited the highest significance for differences in comparisons DKO_R *versus* DKO_{NR} and WT *versus* DKO_{NR}.

Gene symbol	DKO_R - DKO_{NR}	WT - DKO_{NR}	WT - DKO_R	Gene name
Pon2	8.92E-198	9.47E-179	0.04	Paraoxonase2
Ankrd1	5.01E-113	1.36E-110	0.89	Ankyrin repeat domain 1
Igf2bp3	2.88E-99	6.73E-86	0.083	Oncofetal IGF2 mRNA-binding protein 3
Ccnd2	8.17E-97	1.06E-91	0.67	Cyclin D2
Shroom2	1.54E-49	6.45E-53	0.55	Shroom2
Asns	5.78E-46	3.32E-46	1	Aspargine synthetase
Plekha2	2.87E-40	4.68E-28	0.02	Pleckstrin homology domain containing, family A (phosphoinositide binding specific) 2
Lhfpl2	6.10E-39	4.93E-41	0.84	Lipoma HMGIC fusion partner-like 2
Map1b	1.14E-37	2.56E-46	0.18	Microtubule assoc protein 1b
Pon3	1.16E-36	1.78E-41	0.39	Paraoxonase 3
Rhob	4.16E-35	9.71E-37	0.92	RhoB
Prkg2	1.31E-33	2.06E-45	0.07	Protein kinase G 2
Stom	1.54E-32	4.60E-25	0.18	Stomatin
Fbxo17	1.37E-31	6.51E-25	0.08	Fbox protein 17
Cers6	1.61E-30	1.71E-29	0.93	Ceramide synthetase
Aen	2.23E-27	2.54E-21	0.21	Apoptosis enhancing nuclease
Skil	2.77E-27	7.82E-37	0.11	TGFβ/SMAD target gene SKIL
Btbd6	2.97E-27	2.17E-26	0.90	BTB/POZ domain-containing protein 6
Tmem185b	3.63E-27	1.44E-30	0.61	Transmembrane protein 185b
Lamb1	8.05E-27	1.22E-40	0.02	Laminin β1
Cyp4v3	8.13E-27	1.23E-22	0.30	Cytochrome p450 v3
Gfra1	1.23E-26	9.94E-29	0.81	GDNF family receptor α-1
Lrp11	2.06E-26	3.03E-25	0.84	Low density lipoprotein receptor-related protein 11
Zfp185	7.33E-26	1.70E-20	0.23	Zinc finger protein 185
Mtcl1	6.29E-25	5.43E-17	0.03	Microtubule cross-linking factor 1

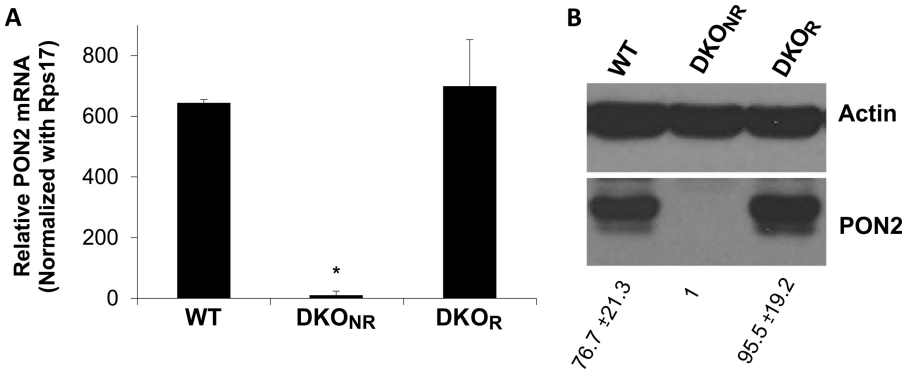

FIGURE 5. **Expression of PON2 in WT and DKO_R but not in DKO_{NR} MEF.** *A,* Q-PCR. *, $p < 0.05$ *versus* WT. *B,* Western blot. Quantitation by densitometry (average ± S.D., $n = 3$) is shown at the *bottom* of the figure. Data are typical of three different experiments in both *A* and *B*.

C12 on Caspase 3/7, $\Delta\psi_{mito}$, and Ca_{cyto} in DKO_{NR} Versus PON2-expressing DKO_{NR} MEF—We tested whether PON2 was required for C12 to activate apoptosis by comparing responses of DKO_{NR} and DKO_{NR} MEF that had been treated with an adenovirus expressing human PON2 or GFP (control). Q-PCR confirmed that DKO_{NR} MEF treated with adenovirus-GFP expressed characteristically low levels of mPON2, whereas adenovirus-hPON2-treated MEF expressed high levels of PON2 (Fig. 6*A*). C12 had no effect on caspase 3/7 activity in DKO_{NR} MEF expressing GFP, whereas C12 caused potent activation of caspase 3/7 in DKO_{NR} MEF expressing hPon2 (Fig. 6*B*).

Previous data showed that one of the earliest responses to C12 in all cell types tested (including both WT and DKO_R MEF) was a slow but persistent depolarization of $\Delta\psi_{mito}$ (9, 23). We tested for C12-induced changes in $\Delta\psi_{mito}$ in DKO_{NR} MEF that had been treated with an adenovirus to express hCFTR (= control) and DKO_{NR} MEF that were treated with adenovirus to express hPON2. Results from these experiments (Fig. 7, *A–C*) showed that C12 had essentially no effect on $\Delta\psi_{mito}$ in DKO_{NR} MEF but caused a slow, persistent and nearly complete depolarization of $\Delta\psi_{mito}$ in DKO_{NR} MEF that expressed hPON2.

Another early indicator of responses to C12 is the release of Ca^{2+} from the ER into the cytosol (9, 19). This was tested by measuring Ca_{cyto}. These experiments (Fig. 8, *A–C*) showed that C12 caused a small, slow increase in Ca_{cyto} in DKO_{NR} MEF that were treated with an adenovirus to express hCFTR (= control), whereas subsequent addition of thapsigargin (blocks Ca^{2+}-ATPase in the ER) (50) caused a rapid, large increase in Ca_{cyto}. In DKO_{NR} MEF treated with adenovirus to express hPON2, C12 caused an immediate, large increase in Ca_{cyto}, and further addition of thapsigargin did not alter Ca_{cyto}. Data in Fig. 8, *A–C*, were therefore consistent with the idea that C12 had little or no effect to release Ca^{2+} from the thapsigargin-releasable pool in the ER of DKO_{NR} MEF. In contrast, adenoviral-mediated expression of hPON2 caused DKO_{NR} MEF to release Ca^{2+} from the ER into the cytosol in response to C12. Overall, data in

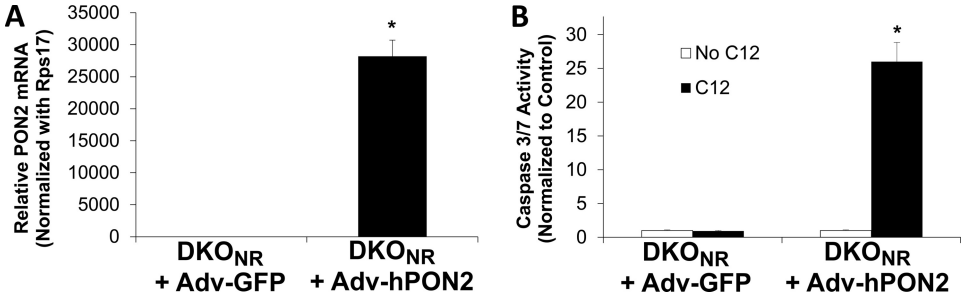

FIGURE 6. **Expression of hPON2 in DKO$_{NR}$ MEF renders them sensitive to C12-induced caspase activation.** *A,* Q-PCR (relative to Rps17) of *PON2* expression in adenovirus (*adv*)-GFP DKO$_{NR}$ and adv-hPON2 DKO$_{NR}$. *, $p < 0.05$ *versus* DKO$_{NR}$ + adenovirus-GFP. *B,* caspase 3/7 activity (in relative light units) in DKO$_{NR}$-GFP and DKO$_{NR}$-hPON2 in response to C12. DKO$_{NR}$-GFP and DKO$_{NR}$-hPON2 MEF were left untreated (control) or treated with C12 (50 μM) for 2 h followed by processing for caspase 3/7 activity. *, $p < 0.05$ *versus* DKO$_{NR}$ + adenovirus-GFP. Data are averages ± S.D. ($n = 3$).

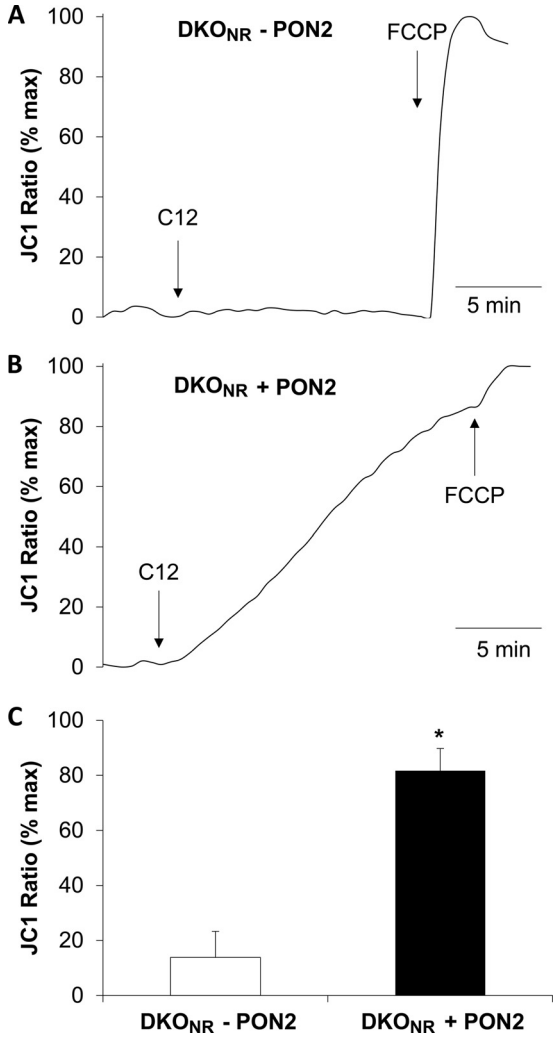

FIGURE 7. **C12 causes depolarization of $\Delta\psi_{mito}$ in hPON2-expressing DKO$_{NR}$ MEF.** DKO$_{NR}$ MEF were treated with either adenovirus-*hCFTR* (serves as control) or adenovirus-*hPON2* and loaded with JC1 (10 μM). $\Delta\psi_{mito}$ was measured from the green/red fluorescence ratio in the imaging microscope during control conditions and following addition of C12 (50 μM) and the protonophore FCCP (10 μM). *A,* C12 caused little effect on $\Delta\psi_{mito}$ of DKO$_{NR}$ MEF that expressed little PON2, and FCCP elicited rapid, maximal depolarization. *B,* C12 caused slow but persistent depolarization of $\Delta\psi_{mito}$ of DKO$_{NR}$ MEF that had been treated with advenovirus-*hPON2*, and FCCP elicited little further depolarization. *C,* summary of effects of C12 on $\Delta\psi_{mito}$ in DKO$_{NR}$-hPON2 and DKO$_{NR}$ + hPON2 MEF. Magnitude of an increase of the JC1 ratio was measured after a 20–25-min treatment with C12 and expressed as percentage of maximal (100%) depolarization with FCCP. Average ± S.D. ($n = 3$, average of >50 cells in each experiment) are shown. *, $p < 0.05$ *versus* DKO$_{NR}$-PON2.

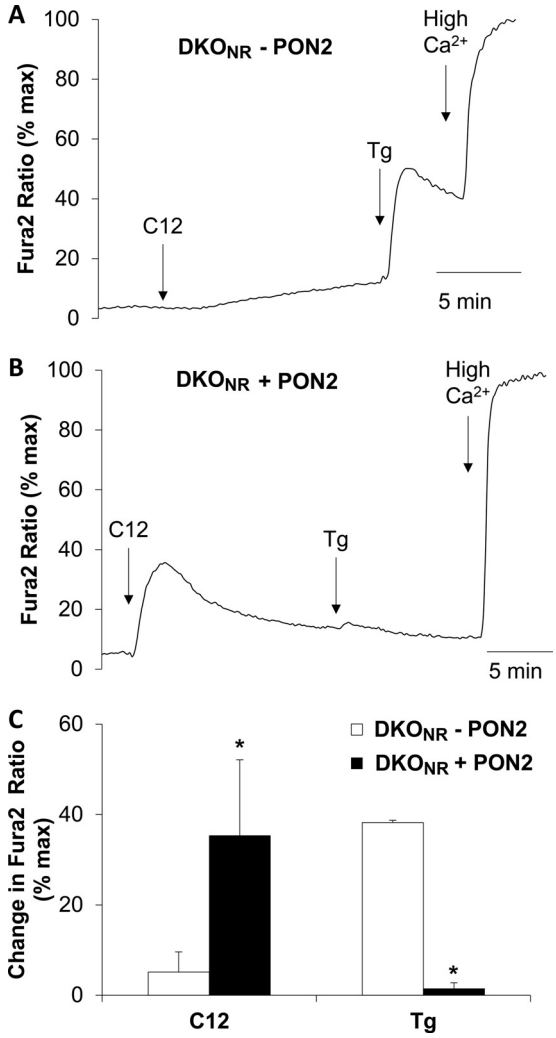

FIGURE 8. **C12 causes increases of Ca$_{cyto}$ in hPON2-expressing DKO$_{NR}$ MEF.** DKO$_{NR}$ MEF were treated with either adenovirus-*hCFTR* (serves as control) or adenovirus-*hPON2* then loaded with fura-2 (5 μM). Ca$_{cyto}$ was measured during control conditions and following addition of C12 (50 μM) and Ca^{2+}-ATPase blocker thapsigargin (1 μM). Data have been presented as percent change of the fura-2 ratio as a percent of maximum in 10 mM Ca^{2+} + ionomycin. *A,* C12 caused little effect on Ca$_{cyto}$ of DKO$_{NR}$ MEF that expressed little hPON2, and thapsigargin elicited a rapid increase in Ca$_{cyto}$. *B,* C12 caused a rapid increase of Ca$_{cyto}$ in DKO$_{NR}$ MEF that had been treated with advenovirus-*hPON2*, and thapsigargin elicited little further increase. *C,* summary of effects of C12 on Ca$_{cyto}$ in DKO$_{NR}$-PON2 and DKO$_{NR}$-PON2 MEF. Magnitude of the increase of the fura-2 ratio was measured after a 15-min treatment with C12 or thapsigargin. Average ± S.D. ($n = 3$, >50 cells in each experiment) are shown. *, $p < 0.05$ *versus* DKO$_{NR}$-PON2.

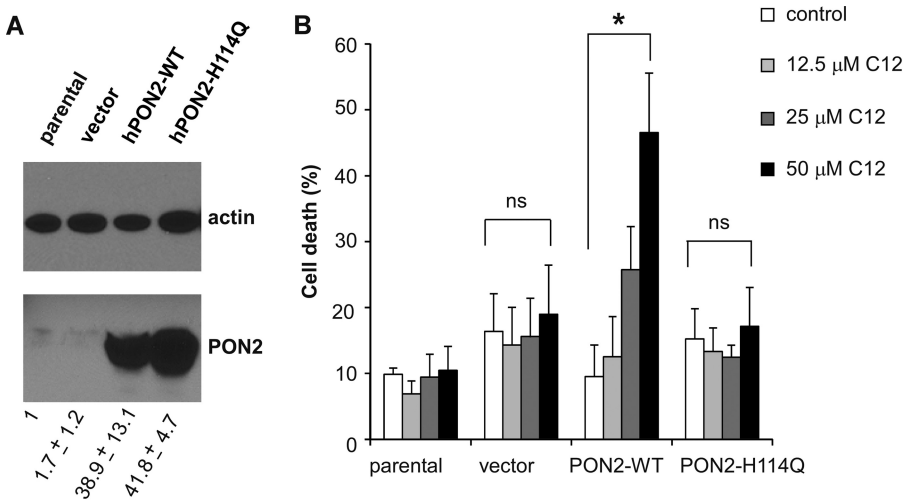

FIGURE 9. **Expression of hPON2 in HEK293T cells renders them sensitive to C12-induced cell killing.** *A,* Western blot of PON2 in HEK293T cells and HEK293T cells expressing vector alone, wild type hPON2, and lactonase mutant hPON2(H114Q). Quantitation by densitometry (average ± S.D., $n = 3$) is shown at the *bottom* of the figure. *B,* cell killing (expressed as percent) of HEK293T, HEK293T (vector), HEK293T-PON2, and HEK-hPON2(H114Q) cells in response to treatment with 0 (control), 12.5, 50, and 100 μM C12 for 24 h followed by processing for PI uptake. *, $p < 0.05$ *versus* control. Data are averages ± S.D. ($n = 3$).

Figs. 6–8 were consistent with the idea that expression of hPON2 in DKO_{NR} MEF caused them to respond to C12 by activating characteristic responses associated with apoptosis: activation of caspase 3/7, depolarization of $\Delta\psi_{mito}$, and release of Ca^{2+} stored in the ER into the cytosol.

PON2-dependent Proapoptotic Effects of C12 on HEK293T Cells—Preliminary experiments indicated that C12 had little effect on the morphology of HEK293T cells. We hypothesized that these cells lacked PON2. Western blots showed that HEK293T cells indeed expressed little PON2 (Fig. 9*A*). These cells were transduced to express empty vector, PON2, or lactonase-deficient mutant PON2(H114Q), and Western blots confirmed that the transduced cells expressed similar levels of wild type PON2 or PON2(H114Q) (Fig. 9*A*).

These cells were also tested for their responses to C12. Killing assays (PI uptake) during treatments with 0 (control), 12.5, 25, and 50 μM C12 showed that compared with responses of vector control HEK293T cells, C12 induced significantly larger, concentration-dependent cell killing in HEK293T-PON2 cells but not in HEK293T cells expressing the lactonase mutant PON2(H114Q) (Fig. 9*B*).

As shown in Fig. 10, C12 (50 μM) similarly caused much larger activation of caspase 3/7 in HEK293T cells expressing wild type PON2 compared with HEK293T cells expressing vector alone or the lactonase mutant PON2(H114Q). C12 also caused a similar activation of caspase 3/7 in vector-treated *versus* untreated HEK293T cells (data not shown).

As shown for individual experiments in Fig. 11, *A–C,* and in the summary in Fig. 11*D*, measurements of $\Delta\psi_{mito}$ with JC-1 showed C12 (50 μM) caused slow, but almost maximal (86%) depolarization of $\Delta\psi_{mito}$ HEK293T cells expressing PON2, but small (17%) depolarization of $\Delta\psi_{mito}$ in HEK293T-vector cells and a 50% depolarization of $\Delta\psi_{mito}$ in HEK293T-PON2(H114Q) cells.

Measurements of Ca_{cyto} showed C12 had only small effects to release Ca^{2+} from the ER into the cytosol in HEK293T-vector and HEK293T-PON2(H114Q) cells but much larger effects in HEK293T-PON2 cells. As shown for individual experiments in

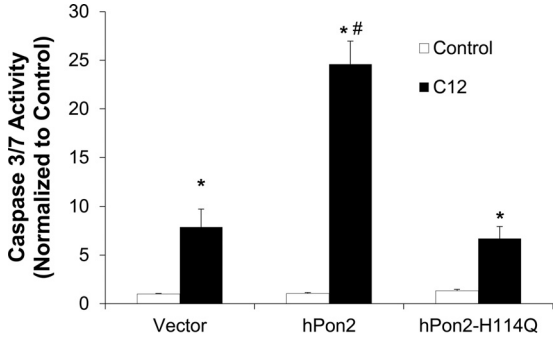

FIGURE 10. **Caspase 3/7 activity (fold-change compared with vector control) in HEK293T-vector, HEK-hPON2, and HEK-hPON2(H114Q) cells in response to C12 (50 μM, 2 h).** *, $p < 0.05$ *versus* control; #, $p < 0.05$ *versus* vector or *versus* PON2-H114Q. Data are averages ± S.D. ($n = 3$).

Fig. 12, *A* and *C*, and summarized in Fig. 12*D*, C12 had essentially no effect on Ca_{cyto}, and subsequent treatment with thapsigargin (1 μM) caused an immediate increase in Ca_{cyto}. In contrast, C12 caused a larger, immediate effect on Ca_{cyto} in HEK293T-PON2 cells, and subsequent treatment with thapsigargin had no effect (Fig. 12, *B* and *D*). These results indicated that C12 released all the Ca^{2+} from the ER in HEK293T-PON2 cells but much less in HEK293T cells expressing vector alone or PON2(H114Q).

DISCUSSION

C12 triggered pro-apoptotic events (activation of caspase 3/7, release of cytochrome c from mitochondria and cell killing) in both WT and DKO_R MEF (23), both of which express high levels of PON2, but not in DKO_{NR} MEF, which express little PON2 (Table 1 and Fig. 5*B*). In contrast, C12 had no effect on DKO_{NR} MEF that expressed very low levels of PON2. In addition, expression of hPON in DKO_{NR} MEF caused these cells to become sensitive to C12: C12 had only small or no effects on $\Delta\psi_{mito}$, Ca^{2+} release from the ER, and activation of caspase 3/7 in DKO_{NR} MEF, but had large effects in DKO_{NR} MEF that expressed PON2. C12 also triggered caspase 3/7 activation, release of Ca^{2+} from the ER, depolarization of $\Delta\psi_{mito}$, and cell

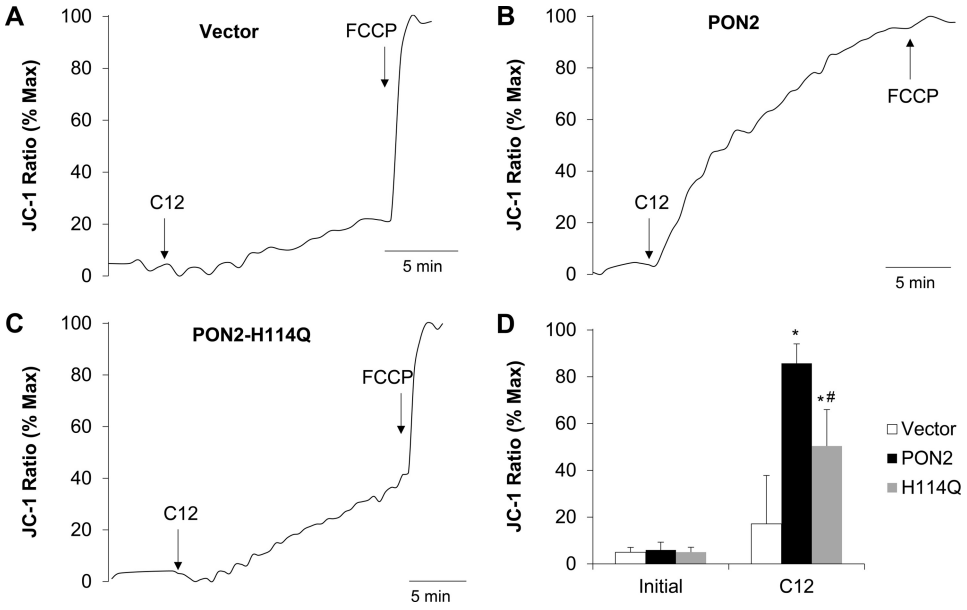

FIGURE 11. **C12 causes depolarization of $\Delta\psi_{mito}$ in HEK293T cells expressing wild type hPON2 but no depolarization in cells expressing vector alone and less depolarization in HEK293T cells expressing hPON2(H114Q).** *A,* results from a typical experiment show that C12 caused little effect on $\Delta\psi_{mito}$ of HEK293T-vector cells, and FCCP elicited rapid, maximal depolarization. *B,* C12 caused a slow, persistent depolarization of $\Delta\psi_{mito}$ of HEK293T-PON2 cells, and FCCP elicited little further depolarization. *C,* C12 caused a slow and less pronounced (*versus* HEK293T-PON2) depolarization of $\Delta\psi_{mito}$ in HEK293T-PON2(H114Q) cells, and FCCP elicited a rapid further depolarization. *D,* summary of effects of C12 on $\Delta\psi_{mito}$ in vector-, hPON2-, and hPON2(H114Q)-HEK293T cells. Magnitude of increase of the JC1 ratio was measured after a 15–20-min treatment with C12 and expressed as the percentage of maximal (100%) depolarization with FCCP. Average ± S.D. (n = 3–5, average of >50 cells in each experiment) are shown. *, $p < 0.05$ *versus* initial; #, $p < 0.05$ *versus* PON2.

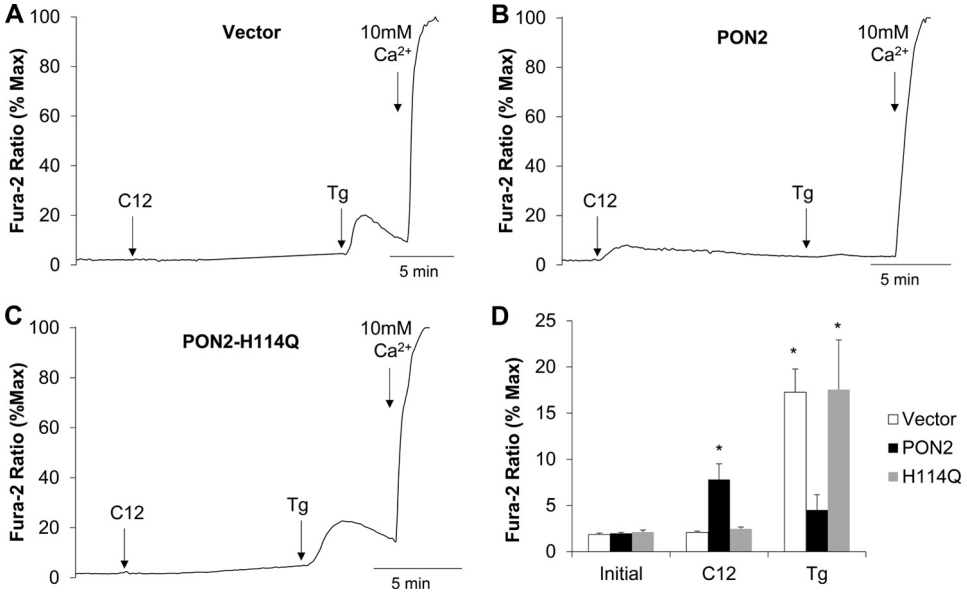

FIGURE 12. **C12 causes ER to release Ca^{2+} in HEK293T-PON2 cells stably expressing hPON2 but not in vector control or hPON2(H114Q)-expressing HEK293T cells.** Ca_{cyto} was measured during control conditions and following addition of C12 (50 μM) and thapsigargin (1 μM) to achieve a maximal release of Ca^{2+} from the ER. Data have been presented as percent change of the fura-2 ratio as a percent of maximum. *A,* C12 caused little effect on Ca_{cyto} of HEK293T cells, and thapsigargin elicited a rapid increase in Ca_{cyto}. *B,* C12 caused a rapid increase of Ca_{cyto} in HEK293T-PON2 cells, and thapsigargin elicited little further increase. *C,* C12 had little effect on Ca_{cyto} of HEK293T-hPON2(H114Q) cells, and thapsigargin elicited little further effect. *D,* summary of effects of C12 on Ca_{cyto} in HEK, HEK-hPON2, and HEK-hPON2(H114Q) cells. The magnitude of the increase of the fura-2 ratio was measured after a 2-min treatment with C12 or thapsigargin and expressed as the percentage of the maximal fura-2 ratio. Average ± S.D. (n = 3, >50 cells in each experiment) are shown. *, $p < 0.05$ *versus* initial.

killing in HEK293T cells that expressed wild type PON2 but had only small or no effects in HEK293T-vector or HEK293T-PON2(H114Q) cells. These data showed that expression of hPON2 with active lactonase activity was required for both human and mouse cells to activate characteristic proapoptotic responses to *N*-(3-oxododecanoyl)-homoserine lactone. The present data along with previous work (23) also showed that this C12-triggered, PON2-dependent apoptosis was unique in that it occurred without the involvement of Bax and Bak. The lack of C12-triggered responses in HEK293T cells transduced with retrovirus to express vector alone and in MEF transduced with adenovirus to express CFTR alone in combination with

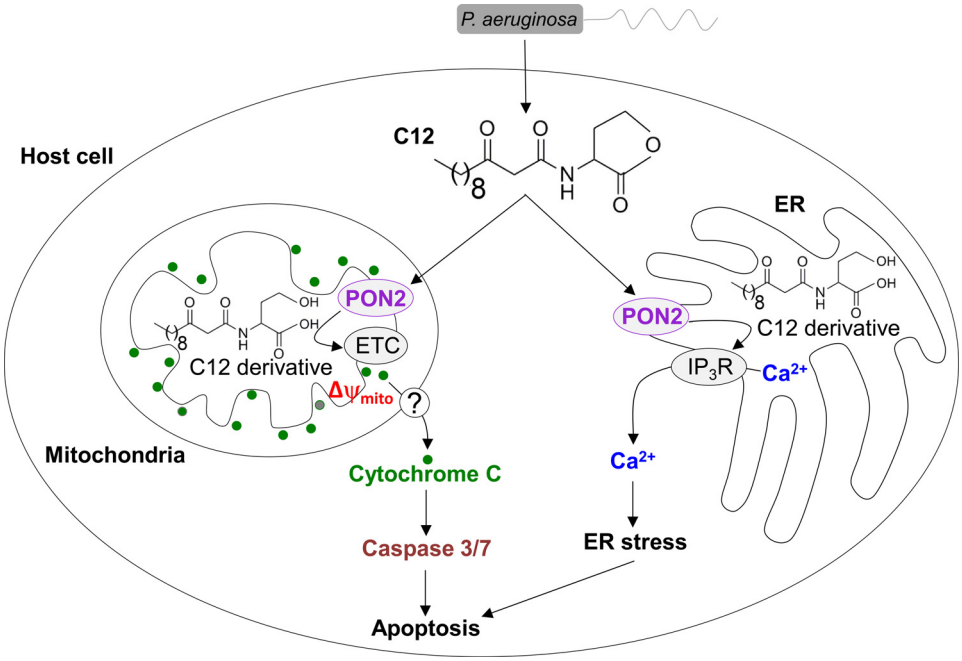

FIGURE 13. **Proposed mechanism for C12-triggered, PON2-mediated activation of early events in ER and mitochondria of host cells.** *P. aeruginosa* produces and releases C12 that enters host cells. PON2 use its lactonase activity to cleave the lactone ring of C12 into the shown derivative. In the ER, the active site of PON2 is located in the ER lumen, so the C12 derivative is produced inside the ER and then activates the inositol trisphosphate receptor to release Ca^{2+} from the ER, leading to ER stress thereby stimulating apoptosis. In the mitochondria PON2 is associated with complex III and coenzyme Q on the inner mitochondrial membrane, and the C12 derivative is predicted to be formed close to and then inhibit the electron transport chain (*ETC*), leading to depolarization of $\Delta\psi_{mito}$, and also cytochrome *c*, leading to its release across the outer mitochondrial membrane through Bax- and Bak-independent mechanisms (shown by ?) into the cytosol to trigger caspase 3 and subsequent apoptostic processes. Because the C12 derivative is highly reactive, it is possible that other derivatives of C12 will also be formed, and these may be the direct activators of events in both the ER and mitochondria.

other data indicated that responses to C12 were mediated through PON2 and that the mode of expression (adenovirus transient *versus* retrovirus stable) and CFTR expression did not alter responses.

Another conclusion from these experiments was that DKO_R and DKO_{NR} MEF expressed a large number of genes differently, even though clonal DKO_R cells were isolated from uncloned DKO_{NR} cells. DKO_R MEF expressed a large number of genes that were cancer- or growth-related, including both *PON2* and *PON3* (32, 37, 38). PON2 is overexpressed in a number of cancers, including leukemia, hepatocellular, and prostate (33–36). DKO_{NR} MEF expressed a mixture of cancer-related genes and other genes related to tissue differentiation and cell-cell signaling. These data showed the danger of assuming that cell lines that have been immortalized by SV40 large T antigen are genetically identical.

The apparent role of PON2 with lactonase activity to mediate or cause apoptosis in response to C12 in host cells was counterintuitive. PON2 appears to be protective against the common proapoptotic agonists doxorubicin and staurosporine and is also up-regulated in many cancers (32, 39, 40). In addition, the lactonase activity of PON2 cleaves C12, so DKO_{NR} MEF (with low PON2) should have been more sensitive to C12, whereas DKO_R (with high PON2) MEF should have been less sensitive to C12. However, the opposite was observed. Previous work (41) showed that inactivation of the lactonase activity of PON2 using PON2(H114Q) did not alter the ability of PON2 to prevent cellular oxidation, and PON2(H114Q) appeared to be more effective than wild type PON2 in preventing apoptosis in response to staurosporine and tunicamycin. Taken together, the present and previous (41) data indicate that PON2 uses its lactonase activity to trigger unique Bax/Bak-independent apoptosis in response to C12, but PON2 uses its lactonase activity to inhibit traditional Bax/Bak-dependent apoptosis in response to tunicamycin and doxorubicin.

PONs 1–3 all hydrolyze lactones and arylesters, although with different specificities (26, 29). It has been proposed that the lactonase activity of PON2 serves an antibacterial function in the lungs and other epithelia that are exposed to bacteria-produced quorum-sensing lactones like C12 (24, 26, 30, 31). Indeed, increases in *PON2* expression in airway epithelial cells lead to hydrolysis and inactivation of C12 in the medium bathing the cells (24, 25). This hydrolysis is expected to reduce quorum-sensing by the bacteria and to reduce responses of host cells to C12. PON2 is thought to have a phospholipase-like structure (28) similar to that of PON1 (27), which may contribute to its ability to cleave a wide range of esters (26, 29).

The molecular mechanism that connects the lactonase activity of PON2 to the unique suite of effects of C12 leading to Bax/Bak-independent apoptosis remains unknown. As summarized in Fig. 13, one possibility that emerges from the present data is that C12 is cleaved by PON2 in the ER (51) and mitochondria (52) into (a) secondary derivative(s) that then has wide-ranging effects. Because the C12 derivative is highly reactive, it is possible that multiple derivatives of C12 will be formed, and these may be the direct activators of multiple events in both the ER and mitochondria. PON2 is reported to localize in the ER with its lactonase and critical Ca^{2+}-binding site, including His-114, oriented toward the lumen (51), so the C12 derivative would be expected to be produced inside the ER

and then activate the inositol trisphosphate receptor (53) directly from the ER face or permeate the ER to act on the cytosolic side of the inositol trisphosphate receptor. Release of Ca^{2+} from the ER will activate ER stress and changes in inflammatory signaling/response (11–16). In mitochondria, PON2 is reported to localize on the inner mitochondrial membrane associated with complex III and coenzyme Q (52), so production of C12 derivatives would be expected to be produced near and then inhibit the electron transport chain and cytochrome *c*. These effects could lead to the observed depolarization of $\Delta\psi_{mito}$ and release and movement of cytochrome *c* from the inner mitochondrial membrane across the outer mitochondrial membrane into the cytosol to activate caspase 3 and downstream effects leading to apoptosis. It is also proposed that the C12 derivative induces pore formation in the outer mitochondrial membrane that mediates movement of cytochrome *c* into the cytosol without involvement of Bax or Bak.

Although speculative, the proposed model provides a useful summary of the data as well as a starting point for further tests of the role of the lactonase activity of PON2 in mediating the effects of C12 on host cells. It will be important to identify and then test the proposed C12 derivatives generated in the ER and mitochondria. Because PON3 was up-regulated in DKO_{NR} and WT MEF compared with DKO_R MEF similar to PON2 (Table 1) and PON3 may serve similar functions as PON2 (31, 32), a direct test of whether PON3 is capable of mediating PON2-like responses to C12 is warranted. Because PON2 is expressed in the airways of CF patients (25, 54) where C12 concentrations may reach high levels, tests of the role of PON2 in lung pathophysiology of CF patients could have important clinical implications.

Acknowledgments—We are grateful to Diana Bautista for suggestions on RNAseq protocols and Justin Choi in the Functional Genome Laboratory for help and advice in running the samples and analyzing the data.

REFERENCES

1. Parsek, M. R., and Greenberg, E. P. (2000) Acyl-homoserine lactone quorum sensing in Gram-negative bacteria: a signaling mechanism involved in associations with higher organisms. *Proc. Natl. Acad. Sci. U.S.A.* **97,** 8789–8793
2. Shiner, E. K., Rumbaugh, K. P., and Williams, S. C. (2005) Inter-kingdom signaling: deciphering the language of acyl homoserine lactones. *FEMS Microbiol Rev.* **29,** 935–947
3. Rumbaugh, K. P., Griswold, J. A., and Hamood, A. N. (2000) The role of quorum sensing in the *in vivo* virulence of *Pseudomonas aeruginosa*. *Microbes Infect.* **2,** 1721–1731
4. Bjarnsholt, T., Ciofu, O., Molin, S., Givskov, M., and Høiby, N. (2013) Applying insights from biofilm biology to drug development: can a new approach be developed? *Nat. Rev. Drug Discov.* **12,** 791–808
5. Staudinger, B. J., Muller, J. F., Halldórsson, S., Boles, B., Angermeyer, A., Nguyen, D., Rosen, H., Baldursson, O., Gottfreðsson, M., Guðmundsson, G. H., and Singh, P. K. (2014) Conditions associated with the cystic fibrosis defect promote chronic Pseudomonas aeruginosa infection. *Am. J. Respir. Crit. Care Med.* **189,** 812–824
6. Kirisits, M. J., and Parsek, M. R. (2006) Does *Pseudomonas aeruginosa* use intercellular signalling to build biofilm communities? *Cell Microbiol.* **8,** 1841–1849
7. Chambers, C. E., Visser, M. B., Schwab, U., and Sokol, P. A. (2005) Identification of *N*-acylhomoserine lactones in mucopurulent respiratory secretions from cystic fibrosis patients. *FEMS Microbiol. Lett.* **244,** 297–304
8. Charlton, T. S., de Nys, R., Netting, A., Kumar, N., Hentzer, M., Givskov, M., and Kjelleberg, S. (2000) A novel and sensitive method for the quantification of *N*-3-oxoacyl homoserine lactones using gas chromatography-mass spectrometry: application to a model bacterial biofilm. *Environ. Microbiol.* **2,** 530–541
9. Schwarzer, C., Fu, Z., Patanwala, M., Hum, L., Lopez-Guzman, M., Illek, B., Kong, W., Lynch, S. V., and Machen, T. E. (2012) *Pseudomonas aeruginosa* biofilm-associated homoserine lactone C12 rapidly activates apoptosis in airway epithelia. *Cell Microbiol.* **14,** 698–709
10. Williams, S. C., Patterson, E. K., Carty, N. L., Griswold, J. A., Hamood, A. N., and Rumbaugh, K. P. (2004) *Pseudomonas aeruginosa* autoinducer enters and functions in mammalian cells. *J. Bacteriol.* **186,** 2281–2287
11. Smith, R. S., Fedyk, E. R., Springer, T. A., Mukaida, N., Iglewski, B. H., and Phipps, R. P. (2001) IL-8 production in human lung fibroblasts and epithelial cells activated by the *Pseudomonas* autoinducer *N*-3-oxododecanoyl homoserine lactone is transcriptionally regulated by NF-κB and activator protein-2. *J. Immunol.* **167,** 366–374
12. DiMango, E., Zar, H. J., Bryan, R., and Prince, A. (1995) Diverse *Pseudomonas aeruginosa* gene products stimulate respiratory epithelial cells to produce interleukin-8. *J. Clin. Invest.* **96,** 2204–2210
13. Telford, G., Wheeler, D., Williams, P., Tomkins, P. T., Appleby, P., Sewell, H., Stewart, G. S., Bycroft, B. W., and Pritchard, D. I. (1998) The *Pseudomonas aeruginosa* quorum-sensing signal molecule *N*-(3-oxododecanoyl)-L-homoserine lactone has immunomodulatory activity. *Infect. Immun.* **66,** 36–42
14. Kravchenko, V. V., Kaufmann, G. F., Mathison, J. C., Scott, D. A., Katz, A. Z., Grauer, D. C., Lehmann, M., Meijler, M. M., Janda, K. D., and Ulevitch, R. J. (2008) Modulation of gene expression via disruption of NF-κB signaling by a bacterial small molecule. *Science* **321,** 259–263
15. Valentine, C. D., Zhang, H., Phuan, P. W., Nguyen, J., Verkman, A. S., and Haggie, P. M. (2014) Small molecule screen yields inhibitors of *Pseudomonas* homoserine lactone-induced host responses. *Cell Microbiol.* **16,** 1–14
16. Grabiner, M. A., Fu, Z., Wu, T., Barry, K. C., Schwarzer, C., and Machen, T. E. (2014) Pseudomonas aeruginosa quorum-sensing molecule homoserine lactone modulates inflammatory signaling through PERK and eIF2α. *J. Immunol.* **193,** 1459–1467
17. Tateda, K., Ishii, Y., Horikawa, M., Matsumoto, T., Miyairi, S., Pechere, J. C., Standiford, T. J., Ishiguro, M., and Yamaguchi, K. (2003) The *Pseudomonas aeruginosa* autoinducer *N*-3-oxododecanoyl homoserine lactone accelerates apoptosis in macrophages and neutrophils. *Infect. Immun.* **71,** 5785–5793
18. Li, L., Hooi, D., Chhabra, S. R., Pritchard, D., and Shaw, P. E. (2004) Bacterial *N*-acylhomoserine lactone-induced apoptosis in breast carcinoma cells correlated with down-modulation of STAT3. *Oncogene* **23,** 4894–4902
19. Shiner, E. K., Terentyev, D., Bryan, A., Sennoune, S., Martinez-Zaguilan, R., Li, G., Gyorke, S., Williams, S. C., and Rumbaugh, K. P. (2006) *Pseudomonas aeruginosa* autoinducer modulates host cell responses through calcium signalling. *Cell. Microbiol.* **8,** 1601–1610
20. Jacobi, C. A., Schiffner, F., Henkel, M., Waibel, M., Stork, B., Daubrawa, M., Eberl, L., Gregor, M., and Wesselborg, S. (2009) Effects of bacterial *N*-acylhomoserine lactones on human Jurkat T lymphocytes-OdDHL induces apoptosis via the mitochondrial pathway. *Int. J. Med. Microbiol.* **299,** 509–519
21. Valentine, C. D., Anderson, M. O., Papa, F. R., and Haggie, P. M. (2013) X-box binding protein 1 (XBP1s) is a critical determinant of *Pseudomonas aeruginosa* homoserine lactone-mediated apoptosis. *PLoS Pathog.* **9,** e1003576
22. Schwarzer, C., Ravishankar, B., Patanwala, M., Shuai, S., Fu, Z., Illek, B., Fischer, H., and Machen, T. E. (2014) Thapsigargin blocks *Pseudomonas aeruginosa* homoserine lactone-induced apoptosis in airway epithelia. *Am. J. Physiol. Cell Physiol.* **306,** C844–55
23. Schwarzer, C., Fu, Z., Shuai, S., Babbar, S., Zhao, G., Li, C., and Machen, T. E. (2014) *Pseudomonas aeruginosa* homoserine lactone triggers apoptosis and Bak/Bax-independent release of mitochondrial cytochrome *c* in fibroblasts. *Cell Microbiol.* **16,** 1094–1104
24. Chun, C. K., Ozer, E. A., Welsh, M. J., Zabner, J., and Greenberg, E. P.

(2004) Inactivation of a *Pseudomonas aeruginosa* quorum-sensing signal by human airway epithelia. *Proc. Natl. Acad. Sci. U.S.A.* **101,** 3587–3590
25. Stoltz, D. A., Ozer, E. A., Ng, C. J., Yu, J. M., Reddy, S. T., Lusis, A. J., Bourquard, N., Parsek, M. R., Zabner, J., and Shih, D. M. (2007) Paraoxonase-2 deficiency enhances *Pseudomonas aeruginosa* quorum sensing in murine tracheal epithelia. *Am. J. Physiol. Lung Cell. Mol. Physiol.* **292,** L852–60
26. Bar-Rogovsky, H., Hugenmatter, A., and Tawfik, D. S. (2013) The evolutionary origins of detoxifying enzymes: the mammalian serum paraoxonases (PONs) relate to bacterial homoserine lactonases. *J. Biol. Chem.* **288,** 23914–23927
27. Harel, M., Aharoni, A., Gaidukov, L., Brumshtein, B., Khersonsky, O., Meged, R., Dvir, H., Ravelli, R. B., McCarthy, A., Toker, L., Silman, I., Sussman, J. L., and Tawfik, D. S. (2004) Structure and evolution of the serum paraoxonase family of detoxifying and anti-atherosclerotic enzymes. *Nat. Struct. Mol. Biol.* **11,** 412–419
28. Barathi, S., Charanya, M., Muthukumaran, S., Angayarkanni, N., and Umashankar, V. (2010) Comparative modeling of PON2 and analysis of its substrate binding interactions using computational methods. *J. Ocul. Biol. Dis. Infor.* **3,** 64–72
29. Draganov, D. I., Teiber, J. F., Speelman, A., Osawa, Y., Sunahara, R., and La Du, B. N. (2005) Human paraoxonases (PON1, PON2, and PON3) are lactonases with overlapping and distinct substrate specificities. *J. Lipid Res.* **46,** 1239–1247
30. Teiber, J. F., Horke, S., Haines, D. C., Chowdhary, P. K., Xiao, J., Kramer, G. L., Haley, R. W., and Draganov, D. I. (2008) Dominant role of paraoxonases in inactivation of the *Pseudomonas aeruginosa* quorum-sensing signal *N*-(3-oxododecanoyl)-L-homoserine lactone. *Infect. Immun.* **76,** 2512–2519
31. Schweikert, E. M., Amort, J., Wilgenbus, P., Förstermann, U., Teiber, J. F., and Horke, S. (2012) Paraoxonases-2 and -3 are important defense enzymes against *Pseudomonas aeruginosa* virulence factors due to their antioxidative and anti-Inflammatory properties. *J. Lipids* **2012,** 352857
32. Devarajan, A., Shih, D., and Reddy, S. T. (2014) Inflammation, infection, cancer and all that . . . the role of paraoxonases. *Adv. Exp. Med. Biol.* **824,** 33–41
33. Li, Y., Li, Y., Tang, R., Xu, H., Qiu, M., Chen, Q., Chen, J., Fu, Z., Ying, K., Xie, Y., and Mao, Y. (2002) Discovery and analysis of hepatocellular carcinoma genes using cDNA microarrays. *J. Cancer Res. Clin. Oncol.* **128,** 369–379
34. Ribarska, T., Ingenwerth, M., Goering, W., Engers, R., and Schulz, W. A. (2010) Epigenetic inactivation of the placentally imprinted tumor suppressor gene TFPI2 in prostate carcinoma. *Cancer Genomics Proteomics* **7,** 51–60
35. Ross, M. E., Zhou, X., Song, G., Shurtleff, S. A., Girtman, K., Williams, W. K., Liu, H. C., Mahfouz, R., Raimondi, S. C., Lenny, N., Patel, A., and Downing, J. R. (2003) Classification of pediatric acute lymphoblastic leukemia by gene expression profiling. *Blood* **102,** 2951–2959
36. Frank, O., Brors, B., Fabarius, A., Li, L., Haak, M., Merk, S., Schwindel, U., Zheng, C., Müller, M. C., Gretz, N., Hehlmann, R., Hochhaus, A., and Seifarth, W. (2006) Gene expression signature of primary imatinib-resistant chronic myeloid leukemia patients. *Leukemia* **20,** 1400–1407
37. Pise-Masison, C. A., Radonovich, M., Mahieux, R., Chatterjee, P., Whiteford, C., Duvall, J., Guillerm, C., Gessain, A., and Brady, J. N. (2002) Transcription profile of cells infected with human T-cell leukemia virus type I compared with activated lymphocytes. *Cancer Res.* **62,** 3562–3571
38. Schweikert, E. M., Devarajan, A., Witte, I., Wilgenbus, P., Amort, J., Förstermann, U., Shabazian, A., Grijalva, V., Shih, D. M., Farias-Eisner, R., Teiber, J. F., Reddy, S. T., and Horke, S. (2012) PON3 is upregulated in cancer tissues and protects against mitochondrial superoxide-mediated cell death. *Cell Death Differ.* **19,** 1549–1560
39. Witte, I., Altenhöfer, S., Wilgenbus, P., Amort, J., Clement, A. M., Pautz, A., Li, H., Förestermann, U., and Horke, S. (2011) Beyond reduction of atherosclerosis: PON2 provides apoptosis resistance and stabilizes tumor cells. *Cell Death Dis.* **2,** e112
40. Witte, I., Foerstermann, U., Devarajan, A., Reddy, S. T., and Horke, S. (2012) Protectors or traitors: the roles of PON2 and PON3 in atherosclerosis and cancer. *J. Lipids.* **2012,** 342806
41. Altenhöfer, S., Witte, I., Teiber, J. F., Wilgenbus, P., Pautz, A., Li, H., Daiber, A., Witan, H., Clement, A. M., Förstermann, U., and Horke, S. (2010) One enzyme, two functions: PON2 prevents mitochondrial superoxide formation and apoptosis independent from its lactonase activity. *J. Biol. Chem.* **285,** 24398–24403
42. Wang, X., Olberding, K. E., White, C., and Li, C. (2011) Bcl-2 proteins regulate ER membrane permeability to luminal proteins during ER stress-induced apoptosis. *Cell Death Differ.* **18,** 38–47
43. Trapnell, C., Pachter, L., Salzberg, S. L. (2009) TopHat: discovering splice junctions with RNA-Seq. *Bioinformatics* 25, 1105–1111
44. Anders, S., Pyl, P. T., and Huber, W. (2014) HTSeq: a Python framework to work with high-throughput sequencing data. *Bioinformatics* **31,** 166–169
45. Anders, S., and Huber, W. (2010) Differential expression analysis for sequence count data. *Genome Biol.* **11,** R106
46. Hybiske, K., Fu, Z., Schwarzer, C., Tseng, J., Do, J., Huang, N., and Machen, T. E. (2007) Effects of cystic fibrosis transmembrane conductance regulator and δF508CFTR on inflammatory response, ER stress, and Ca^{2+} of airway epithelia. *Am. J. Physiol. Lung Cell. Mol. Physiol.* **293,** L1250-L1260
47. Schwarzer, C., Fu, Z., Fischer, H., and Machen, T. E. (2008) Redox-independent activation of NF-κB by *Pseudomonas aeruginosa* pyocyanin in a cystic fibrosis airway epithelial cell line. *J. Biol. Chem.* **283,** 27144–27153
48. Grynkiewicz, G., Poenie, M., and Tsien, R. Y. (1985) A new generation of Ca^{2+} indicators with greatly improved fluorescence properties. *J. Biol. Chem.* **260,** 3440–3450
49. Horke, S., Witte, I., Altenhöfer, S., Wilgenbus, P., Goldeck, M., Förstermann, U., Xiao, J., Kramer, G. L., Haines, D. C., Chowdhary, P. K., Haley, R. W., and Teiber, J. F. (2010) Paraoxonase 2 is down-regulated by the *Pseudomonas aeruginosa* quorumsensing signal *N*-(3-oxododecanoyl)-L-homoserine lactone and attenuates oxidative stress induced by pyocyanin. *Biochem. J.* **426,** 73–83
50. Christensen, S. B., Andersen, A., Poulsen, J. C., and Treiman, M. (1993) Derivatives of thapsigargin as probes of its binding site on endoplasmic reticulum Ca^{2}-ATPase: stereoselectivity and important functional groups. *FEBS Lett.* **335,** 345–348
51. Hagmann, H., Kuczkowski, A., Ruehl, M., Lamkemeyer, T., Brodesser, S., Horke, S., Dryer, S., Schermer, B., Benzing, T., and Brinkkoetter, P. T. (2014) Breaking the chain at the membrane: paraoxonase 2 counteracts lipid peroxidation at the plasma membrane. *FASEB J.* **28,** 1769–1779
52. Devarajan, A., Bourquard, N., Hama, S., Navab, M., Grijalva, V. R., Morvardi, S., Clarke, C. F., Vergnes, L., Reue, K., Teiber, J. F., and Reddy, S. T. (2011) Paraoxonase 2 deficiency alters mitochondrial function and exacerbates the development of atherosclerosis. *Antioxid. Redox Signal.* **14,** 341–351
53. Schwarzer, C., Wong, S., Shi, J., Matthes, E., Illek, B., Ianowski, J. P., Arant, R. J., Isacoff, E., Vais, H., Foskett, J. K., Maiellaro, I., Hofer, A. M., and Machen, T. E. (2010) *Pseudomonas aeruginosa* homoserine lactone activates store-operated cAMP and cystic fibrosis transmembrane regulator-dependent Cl^{-} secretion by human airway epithelia. *J. Biol. Chem.* **285,** 34850–34863
54. Griffin, P. E., Roddam, L. F., Belessis, Y. C., Strachan, R., Beggs, S., Jaffe, A., and Cooley, M. A. (2012) Expression of PPARγ and paraoxonase 2 correlated with *Pseudomonas aeruginosa* infection in cystic fibrosis. *PLoS One* **7,** e42241